

Antineoplastic Agents. 499. Synthesis of Hystatin 2 and Related 1*H*-Benzo[*de*][1,6]-naphthyridinium Salts from Aaptamine¹

George R. Pettit,^{*,†} Holger Hoffmann,[†] Delbert L. Herald,[†] Peter M. Blumberg,[‡] Ernest Hamel,[§] Jean M. Schmidt,[†] Yung Chang,[†] Robin K. Pettit,[†] Nancy E. Lewin,[‡] and Larry V. Pearce[‡]

Cancer Research Institute and Department of Chemistry and Biochemistry, and Department of Microbiology, Arizona State University, Box 872404, Tempe, Arizona 85287-2404; Molecular Mechanisms of Tumor Promotion Section, LCCTP, National Cancer Institute, Bethesda, Maryland 20892-4255; and Screening Technologies Branch, Developmental Therapeutics Program, Division of Cancer Treatment, National Cancer Institute at Frederick, National Institutes of Health, Frederick, Maryland 21702

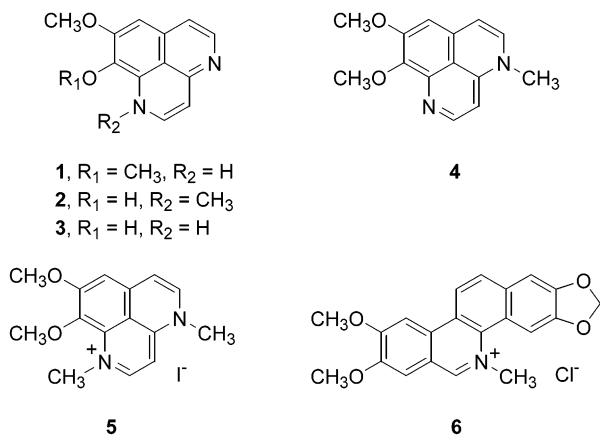
Received February 11, 2003

The marine sponge constituent aaptamine (**1**) has been converted to the cancer cell growth inhibitor and antibiotic designated hystatin 2 (**8a**). Herein, we also report results of an initial SAR evaluation of new benzyl derivatives of aaptamine (**1**). Single benzylation was found to occur at nitrogen N-4 and led to the formation of the 4-benzylaaptamine derivatives **7a–c**, whereas double benzylation gave the quaternary 1*H*-benzo[*de*][1,6]-naphthyridinium salts **8a–c**. The anticancer and antimicrobial properties of these aaptamine derivatives are described. The quaternary ammonium salts **8a** (hystatin 2) and **8b** exhibited significant inhibitory activity against the murine P388 lymphocytic leukemia and a minipanel of human cancer cell lines. Salts **8a** and **8b** also had broad spectrum antimicrobial activities and were most potent against *Mycobacterium tuberculosis*, *Neisseria gonorrhoeae*, and *Micrococcus luteus*. Naphthyridinium chloride **8a** was selected for further development, and results of an initial cell cycle analysis and a cDNA microarray study showed effects consistent with inhibition of the S-phase of cell growth.

The isolation and structural determination of new anticancer constituents from marine invertebrates continue to increase. Recent examples include the nitrogen heterocyclic constituents diazonamide A,² bengamide B,³ makaluvamine P,⁴ spongidepsin,⁵ *N*-methyl-*epi*-manzamine D,⁶ amphiasterin A3,⁷ and pyrinodemins B–D.⁸ The aaptamines form a small group of 1*H*-benzo[*de*]-[1,6]-naphthyridine marine alkaloids with cancer cell growth inhibitory properties. The parent aaptamine (**1**) was first isolated by Nakamura⁹ and was found to possess antineoplastic as well as α -adrenoreceptor blocking activity.¹⁰ The isolation of isoaaptamine (**2**) was first reported by Fedoreev from a sponge in the genus *Suberites*.¹¹ Later, it was isolated by three other groups.^{12–14} Isoaaptamine (**2**) has been reported to be a PKC inhibitor,¹⁵ to possess activity against a number of clinically important microorganisms,¹⁶ and to inhibit growth of cancer cells.¹⁷ In our laboratory, isoaaptamine (**2**) showed significant cytotoxicity against the murine P388 lymphocytic leukemia cell line (ED₅₀ = 0.28 μ g/mL) and against a panel of six human cancer cell lines.¹⁶ Because of the interesting biological activities of isoaaptamine (**2**), we started an extended chemical (SAR) and biological study of the aaptamines.

Several total syntheses of aaptamine (**1**) (for a review, see ref 18) and a synthesis of isoaaptamine¹⁹ have been reported. Due to our multigram isolation of aaptamine from *Hymeniacidon* sp.,¹⁴ this naphthyridine was employed as the starting material for our SAR studies.

Scheme 1



Previously, we described the synthetic conversion of aaptamine (**1**) to isoaaptamine (**2**) and 9-demethyl-aaptamine (**3**).¹⁶ Methylation of aaptamine (**1**) led to the formation of methylaaptamine (**4**). However, the methyl group proved to be bonded to the nitrogen atom at N-4, as shown in (**4**), and not as expected, at N-1. Further methylation led to the formation of 1*H*-benzo[*de*][1,6]-naphthyridinium salt **5**, where both nitrogen atoms N-1 and N-4 were methylated.

The 1*H*-benzo[*de*][1,6]-naphthyridine skeleton of aaptamine (**1**) consists of a quinoline as well as isoquinoline substructure. Interestingly, quaternary isoquinolinium²⁰ or even quinolinium alkaloids²¹ are not unusual in nature and often have biological activity.^{22,23} For example, the alkaloid nitidine (**6**), from the roots of *Toddalia asiatica*, showed significant anti-HIV activity and inhibited HIV reverse transcriptase,^{24,25} whereas

* To whom correspondence should be addressed. Tel.: (480) 965-3351. Fax: (480) 965-8558.

[†] Arizona State University.

[‡] LCCTP, NCI.

[§] STB, NCI.

the structurally related benzo[*c*]phenanthridine alkaloid NK109 showed anticancer activity.²⁶ Because of such considerations and the cancer cell growth inhibitory activity of the quaternary ammonium salt **5** (ED₅₀ 3.9 μg/mL, murine P388), we began a structural investigation of naphthyridine quaternary ammonium salts. Herein we describe the syntheses of 4-benzylaaptamine derivatives **7a–c** and 1*H*-benzo[*de*][1,6]-naphthyridinium salts **8a–c**, all readily prepared from aaptamine (**1**).

Experimental Section

Commercially available reagents were obtained from Sigma-Aldrich Company, and solvents were distilled prior to use. Aaptamine (**1**) was isolated from *Hymeniacion* sp. as previously described.¹⁴ The benzyl bromides were prepared according to a synthesis of 3,4,5-trimethoxybenzyl bromide described previously.²⁷ Column chromatography was performed either using flash silica gel from EM Science (230–400 mesh ASTM) or gravity silica (70–230 mesh ASTM), aluminum oxide from Aldrich (activated, neutral, Bockmann I, ~150 mesh, 58 D), and Sephadex LH-20 from Pharmacia Fine Chemical AB (25–100 μm). Thin-layer chromatography was performed using aluminum oxide plastic sheets (E. Merck). All compounds were visible under UV light (254 nm). Melting points were recorded employing an Electrothermal 9100 apparatus and are uncorrected. The ¹H and ¹³C spectra were obtained using Varian VXR-500 or VXR 400 instruments. Mass spectral data were recorded using a Varian MAT 312 instrument (EIMS), and IR spectra were determined with a Mattson Instruments 2020 Galaxy Series FTIR instrument. All X-ray structure determinations were performed on a Bruker AXS SMART 6000 diffractometer.

General Procedure for the Synthesis of Naphthyridines 7a–c. Under an argon atmosphere, natural aaptamine hydrochloride (**1**, 1.00 g, 3.78 mmol) was suspended in anhydrous tetrahydrofuran (20 mL), and sodium hexamethyldisilazane (7.94 mL, 7.94 mmol, 1.0 M in THF) was added at room temperature. The mixture was stirred for 15 min at the same temperature and then cooled to –78 °C. A solution of the required benzyl bromide (4.54 mmol) in anhydrous tetrahydrofuran (5 mL) was added (dropwise by syringe), and the mixture was stirred for 3 h at –78 °C. Afterward, the mixture was allowed to warm to room temperature and stirred for another 1 h. The reaction was terminated with a 1.0 M HCl solution (10 mL), and the solvent was removed in vacuo. The residue was purified by column chromatography (silica gel, CH₂Cl₂–CH₃OH 6:1). Analytically pure samples were obtained by crystallization from ethyl acetate–methanol using slow evaporation of the solvent.

4-Benzyl-8,9-dimethoxy-4*H*-benzo[*de*][1,6]naphthyridine Hydrochloride (7a). Product: 0.80 g (59%); mp 137–142 °C (dec); *R*_f 0.80 (CH₂Cl₂–CH₃OH 10:1); UV (CH₃OH) λ_{max} (log ε) 207 (4.18), 217 (4.17), 239 (4.21), 259 (4.22), 268 (4.18), 278 (4.15), 357 (3.51), 394 (3.52); IR (KBr) ν_{max} 1651, 1597, 1321, 1248, 1091; ¹H NMR (500 MHz, CD₃OD) δ 3.91 (s, 3H, OCH₃), 4.03 (s, 3H, OCH₃), 5.27 (s, 2H, NCH₂), 6.37 (d, *J* = 7.0 Hz, 1H, H-3), 6.92 (d, *J* = 7.5 Hz, 1H, H-6), 7.08 (d, *J* = 1.5 Hz, 1H, H-7), 7.33–7.29 (m, 3H), 7.39–7.36 (m, 5H, C_{ar}), 7.42 (d, *J* = 7.5 Hz, 1H, H-5), 7.83 (d, *J* = 7.5 Hz, 1H, H-2); ¹³C NMR (126 MHz, CD₃OD) δ 57.14, 57.28, 61.29, 98.11, 102.91, 114.98, 118.78, 128.13, 129.49, 130.30, 132.70, 134.02, 135.37, 135.39, 135.75, 143.78, 151.54, 158.16; EIMS *m/z* 318 (47) [M⁺ – HCl], 303 (12), 289 (10), 227 (50), 213 (11), 199 (15), 184 (22), 167 (14), 91 (100), 65 (13), 28 (55). Anal. Calcd for C, H, N. Found: C.

8,9-Dimethoxy-4-(4-methoxybenzyl)-4*H*-benzo[*de*][1,6]-naphthyridine Hydrochloride (7b). Yield: 0.95 g (65%); mp 235–237 °C (dec); *R*_f 0.81 (CH₂Cl₂–CH₃OH 10:1); UV (CH₃OH) λ_{max} (log ε) 205 (3.97), 241 (4.04), 261 (4.13), 269 (4.14), 359 (3.26), 395 (3.26); IR (KBr) ν_{max} 2839, 1649, 1595, 1516, 1325, 1250, 1089; ¹H NMR (500 MHz, CD₃OD) δ 3.76

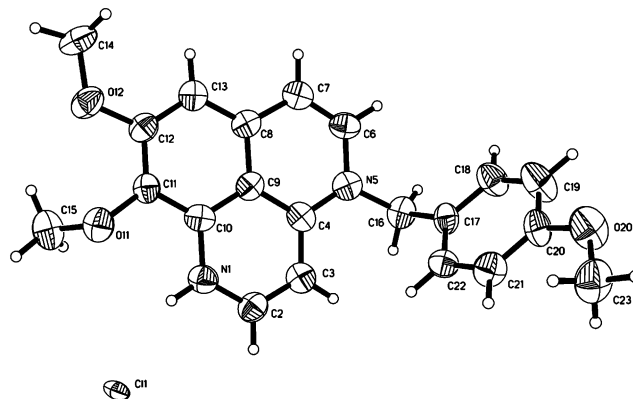


Figure 1. A 50% thermal probability plot of the 4-(4-methoxybenzyl) derivative **7b**.

(s, 3H, OCH₃), 3.93 (s, 3H, OCH₃), 4.05 (s, 3H, OCH₃), 5.21 (s, 2H, NCH₂), 6.45 (d, *J* = 7.3 Hz, 1H, H-3), 6.94 (d, *J* = 9.0 Hz, 2H, C_{ar}), 6.97 (d, *J* = 7.5 Hz, 1H, H-6), 7.14 (s, 1H, H-7), 7.25 (d, *J* = 8.5 Hz, 2H, C_{ar}), 7.45 (d, *J* = 7.5 Hz, 1H, H-5), 7.83 (d, *J* = 7.3 Hz, 1H, H-2); ¹³C NMR (126 MHz, CD₃OD) δ 55.80, 56.96, 57.10, 61.28, 98.15, 102.92, 115.21, 115.68, 118.89, 127.02, 129.69, 132.90, 133.89, 134.98, 135.63, 143.24, 151.72, 158.41, 161.35; EIMS *m/z* 348 (27) [M⁺ – HCl], 227 (11), 167 (60), 121 (100), 33 (10), 28 (50).

X-ray Crystal Structure Determination (7b). 8,9-Dimethoxy-4-(4-methoxybenzyl)-4*H*-benzo[*de*][1,6]naphthyridinium chloride (**7b**): A thin, pale-yellow, needle-shaped crystal (~0.26 × 0.06 × 0.03 mm), grown from a chloroform–methanol–water solution, was mounted on the tip of a glass fiber. Cell parameter measurements and data collection were performed at 123 ± 2 K on a Bruker SMART 6000 diffractometer. Final cell constants were calculated from a set of 1349 reflections from the actual data collection. Frames of data were collected in the θ range of 4.65 to 68.75° (–16 ≤ *h* ≤ 14, –22 ≤ *k* ≤ 22, –8 ≤ *l* ≤ 8) using 0.396° steps in ω such that a comprehensive coverage of the sphere of reflections was performed. After data collection, an empirical absorption correction was applied with the program SADABS.³⁰ Subsequent statistical analysis of the complete reflection set using the XPREP³¹ program indicated the space group was *P2*₁/*c*.

Crystal data: C₂₁H₂₁ClN₂O₅, *a* = 13.7536(13), *b* = 19.0271(17), *c* = 7.1665(6) Å, β = 98.060(5), *V* = 1856.9(3) Å³, λ = (Cu K α) = 1.54178 Å, ρ_c = 1.377 g cm^{–3} for *Z* = 4 and FW = 384.85, *F*(000) = 808. A total of 9803 reflections were collected, of which 2990 were unique (*R*_{int} = 0.1209), and considered observed (*I*_o > 2σ(*I*_o)). These were used in the subsequent structure solution and refinement with SHELXTL-V5.1.³¹ All non-hydrogen atoms for **7b** were located using the default settings of that program. Hydrogen atoms were placed in calculated positions, assigned thermal parameters equal to either 1.2 or 1.5 (depending upon chemical type) of the *U*_{iso} value of the atom to which they were attached, then both coordinates and thermal values were forced to ride that atom during final cycles of refinement. All non-hydrogen atoms were refined anisotropically in a full-matrix least-squares refinement process. The final standard residual *R*₁ value for the model shown in Figure 1 converged to 0.0860 (for observed data) and 0.1454 (for all data). The corresponding Sheldrick *R* values were *wR*₂ of 0.2255 and 0.2458, respectively, and the GOF = 0.995 for all data. The difference Fourier map showed residual electron density; the largest difference peak and hole being +1.226 and –0.527 e/Å³, respectively. However, all peaks were within 1 Å of chlorine atoms and were consequently attributed to those atoms. Final bond distances and angles were all within acceptable limits.

8,9-Dimethoxy-4-(3,4,5-trimethoxybenzyl)-4*H*-benzo[*de*][1,6]naphthyridine Hydrochloride (7c). Product obtained: 1.0 g (59%); mp 198–200 °C (dec); *R*_f 0.87 (CH₂Cl₂–CH₃OH 10:1); UV (CH₃OH) λ_{max} (log ε) 208 nm (4.56), 240 (4.46), 260 (4.48), 269 (4.45), 360 (3.67), 395 (3.69); IR (KBr)

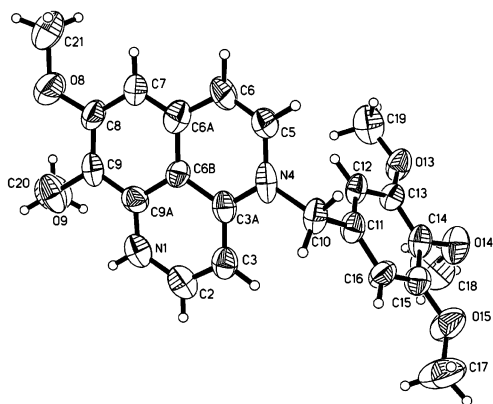


Figure 2. A 40% thermal probability plot of the 4-(3,4,5-trimethoxybenzyl) derivative **7c**.

ν_{\max} 1651, 1593, 1460, 1429, 1321, 1246, 1126, 1091, 999; ^1H NMR (500 MHz, CD_3OD) δ 3.72 (s, 3H, OCH_3), 3.78 (s, 6H, 2 x OCH_3), 3.94 (s, 3H, OCH_3), 4.05 (s, 3H, OCH_3), 5.21 (s, 2H, NCH_2), 6.49 (d, $J = 7.0$ Hz, 1H, H-3), 6.62 (s, 2H, C_{ar}), 6.98 (d, $J = 8.0$ Hz, 1H, H-6), 7.15 (s, 1H, H-7), 7.47 (d, $J = 8.0$ Hz, 1H, H-5), 7.88 (d, $J = 7.0$ Hz, 1H, H-2); ^{13}C NMR (126 MHz, CD_3OD) δ 56.78, 57.13, 57.43, 61.09, 61.30, 98.15, 103.02, 105.71, 115.09, 118.86, 131.25, 132.81, 134.02, 135.19, 135.65, 139.27, 143.56, 151.79, 155.27, 158.38, EIMS m/z 408 (24) [$\text{M}^+ - \text{HCl}$], 181 (100), 28 (46).

X-ray Crystal Structure Determination (7c). 8,9-Dimethoxy-4-(3,4,5-trimethoxybenzyl)-4*H*-benzo[*de*][1,6]-naphthyridin-1-ium chloride (**7c**): A thin plate ($\sim 0.03 \times 0.30 \times 0.32$ mm), grown from a chloroform/methanol/water solution, was mounted on the tip of a glass fiber. Cell parameter measurements and data collection were performed at 298 ± 1 K with a Bruker SMART 6000 diffractometer system using $\text{Cu K}\alpha$ radiation. A sphere of reciprocal space was covered using the MULTIRUN technique.²⁸ Thus, six sets of frames of data were collected with 0.40° steps in ω , and a last set of frames with 0.4° steps in φ , such that 97.5% coverage of all unique reflections to a resolution of 0.84 Å was accomplished.

Crystal data: $\text{C}_{23}\text{H}_{24}\text{ClN}_2\text{O}_5 \cdot 2\text{H}_2\text{O}$ (hydrate), FW = 483.96, monoclinic, $P2_1/n$, $a = 8.3429(5)$, $b = 21.4198(13)$, $c = 28.6694(17)$ Å, $\beta = 92.436(2)^\circ$, $V = 5118.7(5)$ Å³, $Z = 8$, $\rho_c = 1.256$ mg/m³, $\mu(\text{Cu K}\alpha) = 1.688$ mm⁻¹, $\lambda = 1.54178$ Å, $F(000) = 2056$.

A total of 20110 reflections were collected, of which 6738 reflections were independent reflections ($R(\text{int}) = 0.1407$). Subsequent statistical analysis of the data set with the XPREP²⁹ program indicated the spacegroup was $P2_1/n$. Final cell constants were determined from the set of the 2345 observed ($>2\sigma(I)$) reflections which were used in structure solution and refinement. An absorption correction was applied to the data with SADABS.³⁰ Structure determination and refinement was readily accomplished with the direct-methods program SHELXTL.³¹ All non-hydrogen atom coordinates were located in a routine run using default values for that program. The remaining H atom coordinates were calculated at optimum positions. All non-hydrogen atoms were refined anisotropically in a full-matrix least-squares refinement procedure. The H atoms were included, their U_{iso} thermal parameters fixed at either 1.2 or 1.5 (depending on atom type) the value of the U_{iso} of the atom to which they were attached and forced to ride that atom. The final standard residual R_1 value for **7c** was 0.1369 for observed data and 0.2550 for all data. The goodness-of-fit on F^2 was 1.002. The corresponding Sheldrick R values were wR_2 of 0.3624 and 0.3959, respectively. The final model for **7c** is shown in Figure 2. In addition to two parent molecules in the asymmetric cell unit, four molecules of water solvate were also present in each unit. A final difference Fourier map showed some residual electron density, the largest difference peak and hole being +1.712 and -0.551 e/Å³, respectively. However, the principal peaks were within bonding distance of the halide ions and were consequently attributable to these

atoms. Final bond distances and angles were all within expected and acceptable limits.

General Procedure for the Synthesis of 8a–c. Natural aaptamine hydrochloride (**1**, 0.5 g, 1.89 mmol) was dissolved in anhydrous dimethylformamide (50 mL). Potassium carbonate (1.31 g, 9.45 mmol) and the appropriate benzyl bromide (9.45 mmol) were added at room temperature. After being stirred for 12 h at the same temperature, the solution was filtered, and the solvent was removed in vacuo to leave a brown oil. The oily residue was separated by column chromatography (silica gel, $\text{CH}_2\text{Cl}_2/\text{CH}_3\text{OH}$ 6:1) to give the desired products as bright yellow compounds.

1,4-Bis(benzyl)-8,9-dimethoxy-4*H*-benzo[*de*][1,6]-naphthyridin-1-ium Chloride (8a). Isolated yield: 0.63 g (68%); yellow cubes from $\text{EtOAc}-\text{CH}_3\text{OH}$; mp 175°C (dec); R_f 0.69 ($\text{CH}_2\text{Cl}_2/\text{MeOH}$ 10:1); UV (MeOH) λ_{\max} (log ϵ) 207 (4.60), 220 (4.52), 246 (4.53), 262 (4.58), 273 (4.55), 282 (4.55), 416 (4.02); IR (KBr) ν_{\max} 1645, 1568, 1456, 1367, 1338, 1303, 1207, 1157, 1101, 1060, 738; ^1H NMR (500 MHz, CD_3OD) δ 3.56 (s, 3H, OCH_3), 4.01 (s, 3H, OCH_3), 5.38 (s, 2H, NCH_2), 5.71 (s, 2H, NCH_2), 6.52 (d, $J = 8.0$ Hz, 1H, H-3), 7.10 (d, $J = 7.8$ Hz, 1H, H-6), 7.17 (d, $J = 7.5$ Hz, 2H, C_{ar}), 7.23–7.42 (m, 8H, C_{ar}), 7.26 (s, 1H, H-7), 7.59 (d, $J = 7.8$ Hz, 1H, H-5), 7.95 (d, $J = 8.0$ Hz, 1H, H-2); ^{13}C NMR (126 MHz, CD_3OD) δ 57.20, 57.85, 61.46, 62.35, 99.16, 104.36, 115.99, 120.46, 127.21, 128.07, 128.94, 129.60, 129.97, 130.38, 134.25, 134.83, 135.23, 135.71, 136.42, 137.93, 150.57, 150.95, 160.36; EIMS m/z 408 (2) [$\text{M}^+ - \text{HBr}$], 364 (43), 318 (39), 303 (66), 273 (77), 227 (42), 167 (33), 91 (100), 65 (30), 28 (32).

X-ray Crystal Structure Determination (8a). 1,4-Bis(benzyl)-8,9-dimethoxy-4*H*-benzo[*de*][1,6]-naphthyridin-1-ium chloride (**8a**): A thin plate ($\sim 0.40 \times 0.28 \times 0.10$ mm), grown from a chloroform/methanol/water solution, was mounted on the tip of a glass fiber. Cell parameter measurements and data collection were performed at 298 ± 1 K with a Bruker SMART 6000 diffractometer system using $\text{Cu K}\alpha$ radiation. A sphere of reciprocal space was covered using the MULTIRUN technique.²⁸ Thus, six sets of frames of data were collected with 0.40° steps in ω , and a last set of frames with 0.40° steps in φ , such that 93.2% coverage of all unique reflections to a resolution of 0.84 Å was accomplished.

Crystal data: $\text{C}_{27}\text{H}_{25}\text{ClN}_2\text{O}_2 \cdot \text{H}_2\text{O}$ (hydrate), FW = 462.96, triclinic, $P\bar{1}$, $a = 9.35870(10)$, $b = 10.8354(2)$, $c = 11.7009(2)$ Å, $\alpha = 80.7380(10)^\circ$, $\beta = 81.5100(10)^\circ$, $\gamma = 80.9910(10)^\circ$, $V = 1147.46(3)$ Å³, $Z = 2$, $\rho_c = 1.340$ mg/m³, $\mu(\text{Cu K}\alpha) = 1.733$ mm⁻¹, $\lambda = 1.54178$ Å, $F(000) = 488$.

A total of 9247 reflections were collected, of which 4002 reflections were independent reflections ($R(\text{int}) = 0.0807$). Subsequent statistical analysis of the data set with the XPREP²⁹ program indicated the spacegroup was $P\bar{1}$. Final cell constants were determined from the set of the 2877 observed ($>2\sigma(I)$) reflections which were used in structure solution and refinement. An absorption correction was applied to the data with SADABS.³⁰ Structure determination and refinement was readily accomplished with the direct-methods program SHELXTL.³¹ All non-hydrogen atom coordinates were located in a routine run using default values for that program. The remaining H atom coordinates were calculated at optimum positions. All non-hydrogen atoms were refined anisotropically in a full-matrix least-squares refinement procedure. The H atoms were included, their U_{iso} thermal parameters fixed at either 1.2 or 1.5 (depending on atom type) the value of the U_{iso} of the atom to which they were attached and forced to ride that atom. The final standard residual R_1 value for **8a** was 0.0818 for observed data and 0.0972 for all data. The goodness-of-fit on F^2 was 0.997. The corresponding Sheldrick R values were wR_2 of 0.2320 and 0.2478, respectively. The final model for **8a** is shown in Figure 3. In addition to the parent molecule, a molecule of water solvate was also present in the unique cell unit. A final difference Fourier map showed some residual electron density, the largest difference peak and hole being +1.503 and -0.363 e/Å³, respectively. However, the principal peaks were within close proximity of the halide ions and were

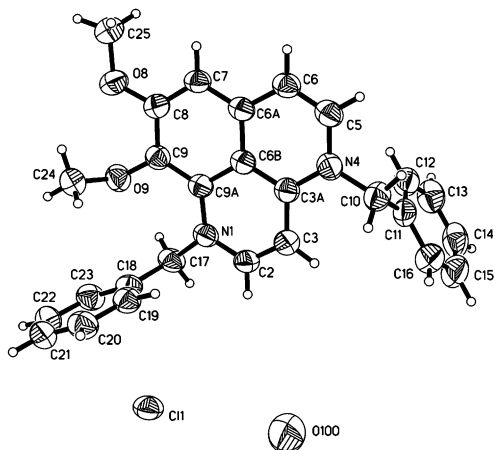


Figure 3. A 50% thermal ellipsoid probability plot showing the molecular contents of the asymmetric cell unit for 1,4-bis-benzyl derivative **8a**.

consequently attributable to these atoms. Final bond distances and angles were all within expected and acceptable limits.

1,4-Bis(4-methoxybenzyl)-8,9-dimethoxy-4H-benzo[de][1,6]naphthyridin-1-ium Bromide (8b). Realized yield: 0.97 g (89%); R_f 0.64 (CH₂Cl₂/CH₃OH 10:1); UV (CH₃OH) λ_{\max} (log ϵ) 209 (4.28), 255 (4.05), 261 (4.08), 273 (4.09), 280 (4.06), 307 (3.45), 316 (3.34), 414 (3.60); IR (KBr) ν_{\max} 1645, 1610, 1566, 1514, 1249; ¹H NMR (500 MHz, CD₃OD) δ 3.64 (s, 3H, OCH₃), 3.72 (s, 3H, OCH₃), 3.76 (s, 3H, OCH₃), 4.02 (s, 3H, OCH₃), 5.26 (s, 2H, NCH₂), 5.64 (s, 2H, NCH₂), 6.54 (d, J = 7.5 Hz, 1H, H-3), 6.85 (d, J = 9.0 Hz, 2H, C_{ar}), 6.94 (d, J = 9.0 Hz, 2H, C_{ar}), 7.06 (d, J = 7.0 Hz, 1H, H-6), 7.13 (d, J = 9.0 Hz, 2H, C_{ar}), 7.24 (s, 1H, H-7), 7.25 (d, J = 10.0 Hz, 2H, C_{ar}), 7.55 (d, J = 7.0 Hz, 1H, H-5), 7.96 (d, J = 7.5 Hz, 1H, H-2); ¹³C NMR (126 MHz, CD₃OD) δ 56.24, 56.33, 57.71, 57.95, 61.37, 62.84, 99.65, 104.73, 115.80, 116.22, 116.37, 120.98, 127.39, 129.60, 130.09, 130.23, 134.79, 135.24, 135.99, 136.90, 150.69, 151.27, 160.83, 161.48, 161.88; EIMS m/z 468 (2) [M⁺ - HBr], 348 (21), 121 (100), 95 (19), 94 (20), 78 (23), 28 (35).

X-ray Crystal Structure Determination (8b). 1,4-Bis-(4-methoxybenzyl)-8,9-dimethoxy-4H-benzo[de][1,6]naphthyridin-1-ium bromide (**8b**): A large, thin plate (~0.30 × 0.30 × 0.20 mm), grown from a chloroform/methanol solution, was mounted on the tip of a glass fiber with Vaseline. Cell parameter measurements and data collection were performed at ambient (27 °C) with a Bruker SMART 6000 diffractometer system using Cu K α radiation. A sphere of reciprocal space was covered using the MULTIRUN technique.²⁸ Thus, six sets of frames of data were collected with 0.396° steps in ω , and a last set of frames with 0.396° steps in φ , such that 98.1% coverage of all unique reflections to a resolution of 0.84 Å was accomplished.

Crystal data: C₂₉H₂₉BrN₂O₄·H₂O (hydrate), FW = 567.47, triclinic, $P\bar{1}$, a = 9.6217(2), b = 10.9327(3), c = 13.4568(3) Å, α = 87.6370(10), β = 86.0040(10), γ = 69.7300(10)°, V = 1324.42(5) Å³, Z = 2, ρ_c = 1.423 mg/m³, μ (Cu K α) = 2.460 mm⁻¹, λ = 1.54178 Å, $F(000)$ = 588.

A total of 9328 reflections were collected, of which 3728 reflections were independent reflections ($R(\text{int})$ = 0.1038). Subsequent statistical analysis of the data set with the XPREP²⁹ program indicated the spacegroup was $C2/c$. Final cell constants were determined from the set of the 2933 observed ($>2\sigma(I)$) reflections which were used in structure solution and refinement. An absorption correction was applied to the data with SADABS.³⁰ Structure determination and refinement was readily accomplished with the direct-methods program SHELXTL.³¹ All non-hydrogen atom coordinates were located in a routine run using default values for that program. The remaining H atom coordinates were calculated at optimum positions. All non-hydrogen atoms were refined anisotropically in a full-matrix least-squares refinement procedure. The H

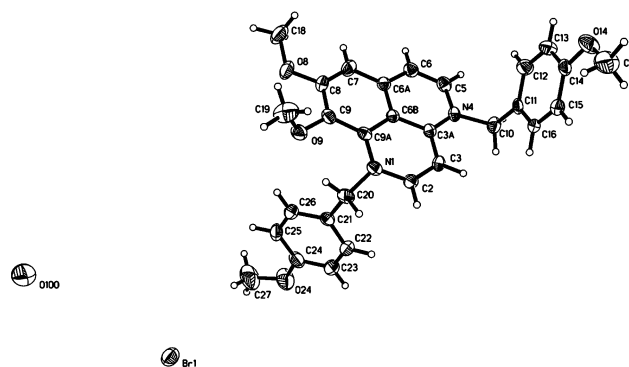


Figure 4. A 50% thermal ellipsoid probability plot showing the contents of the asymmetric cell unit for the 1,4-bis(4-methoxybenzyl) derivative **8b**.

atoms were included, their U_{iso} thermal parameters fixed at either 1.2 or 1.5 (depending on atom type) the value of the U_{iso} of the atom to which they were attached and forced to ride that atom. The final standard residual R_1 value for **8b** was 0.0668 for observed data and 0.0762 for all data. The goodness-of-fit on F^2 was 1.020. The corresponding Sheldrick R values were wR_2 of 0.1672 and 0.1713, respectively. In addition to the parent molecule, a molecule of water was also present in the asymmetric unit. The final model for **8b** is shown in Figure 4. A final difference Fourier map showed some residual electron density, the largest difference peak and hole being +0.637 and -0.875 e/Å³, respectively. However, the principal peaks were within close proximity of the halide ions sites and were consequently attributable to these atoms. Final bond distances and angles were all within expected and acceptable limits.

1,4-Bis(3,4,5-trimethoxybenzyl)-8,9-dimethoxy-4H-benzo[de][1,6]naphthyridin-1-ium Bromide (8c). Final product 1.0 g (79%); mp 116–118 °C; R_f 0.75 (CH₂Cl₂/CH₃OH 10:1); UV (CH₃OH) λ_{\max} (log ϵ) 4.32, 261 (3.99), 273 (3.98), 416 (3.52); IR (KBr) ν_{\max} 1649, 1591, 1568, 1460, 1124; ¹H NMR (500 MHz, CD₃OD) δ 3.69 (s, 3H, OCH₃), 3.70 (s, 3H, OCH₃), 3.71 (s, 3H, OCH₃), 3.73 (s, 3H, OCH₃), 3.77 (s, 6H, OCH₃), 4.05 (s, 3H, OCH₃), 5.29 (s, 2H, NCH₂), 5.65 (s, 2H, NCH₂), 6.51 (s, 2H, C_{ar}), 6.61 (s, 2H, C_{ar}), 6.60 (d, J = 7.5 Hz, 1H, H-3), 7.11 (d, J = 7.5 Hz, 1H, H-6), 7.29 (s, 1H, H-7), 7.61 (d, J = 7.5 Hz, 1H, H-5), 8.02 (d, J = 7.5 Hz, 1H, H-2); ¹³C NMR (126 MHz, CD₃OD) δ 57.18, 57.29, 57.78, 58.52, 61.59, 61.67, 62.87, 99.86, 104.89, 105.89, 106.27, 116.44, 120.87, 131.58, 134.02, 134.81, 135.26, 136.12, 137.02, 139.48, 139.82, 150.76, 151.35, 155.47, 155.80, 160.94; EIMS m/z 588 (1) [M⁺ - HBr], 408 (11), 181 (100), 95 (22), 94 (23), 28 (32).

X-ray Crystal Structure Determination (8c). 1,4-Bis-(3,4,5-trimethoxybenzyl)-8,9-dimethoxy-4H-benzo[de][1,6]naphthyridin-1-ium bromide (**8c**): A large, thin plate (~0.8 × 0.42 × 0.06 mm), grown from a methanol/water solution, was mounted on the tip of a glass fiber with Vaseline. Cell parameter measurements and data collection were performed at 123 K (-150 °C) with a Bruker SMART 6000 diffractometer system using Cu K α radiation. A sphere of reciprocal space was covered using the MULTIRUN technique.²⁸ Thus, six sets of frames of data were collected with 0.396° steps in ω , and a last set of frames with 0.396° steps in φ , such that 96.4% coverage of all unique reflections to a resolution of 0.84 Å was accomplished.

Crystal data: C₃₃H₃₇BrN₂O₈·2H₂O (hydrate), FW = 705.59, monoclinic, $C2/c$, a = 24.9554(6), b = 12.9354(3), c = 22.1264(5) Å, β = 116.0810(10)°, V = 6415.3(3) Å³, Z = 8, ρ_c = 1.461 mg/m³, μ (Cu K α) = 2.267 mm⁻¹, λ = 1.54178 Å, $F(000)$ = 2944.

A total of 23034 reflections were collected, of which 5828 reflections were independent reflections ($R(\text{int})$ = 0.0610). Subsequent statistical analysis of the data set with the XPREP²⁹ program indicated the spacegroup was $C2/c$. Final cell constants were determined from the set of the 4827 observed ($>2\sigma(I)$) reflections which were used in structure

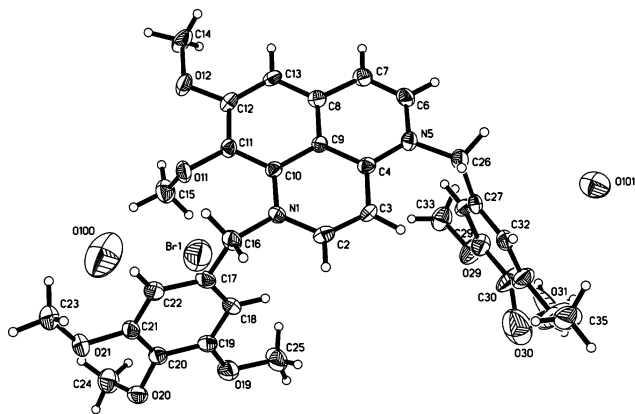


Figure 5. A 50% probability ellipsoid plot showing the molecular contents of the asymmetric cell unit for the 1,4-bis-(trimethoxybenzyl) derivative **8c**.

solution and refinement. An absorption correction was applied to the data with SADABS.³⁰ Structure determination and refinement was readily accomplished with the direct-methods program SHELXTL.³¹ All non-hydrogen atom coordinates were located in a routine run using default values for that program. The remaining H atom coordinates were calculated at optimum positions. All non-hydrogen atoms were refined anisotropically in a full-matrix least-squares refinement procedure. The H atoms were included, their U_{iso} thermal parameters fixed at either 1.2 or 1.5 (depending on atom type) the value of the U_{iso} of the atom to which they were attached and forced to ride that atom. The final standard residual R_1 value for **8c** was 0.0848 for observed data and 0.1019 for all data. The goodness-of-fit on F^2 was 0.997. The corresponding Sheldrick R values were wR_2 of 0.2185 and 0.2364, respectively. In addition to the parent molecule, two molecules of water hydrate were found in the asymmetric unit. The final model for **8c** is shown in Figure 5. A final difference Fourier map showed some residual electron density; the largest difference peak and hole being +1.720 and -0.449 $e\text{\AA}^{-3}$, respectively. However, the principal peaks were within close proximity of the halide ions and were consequently attributable to these atoms. Final bond distances and angles were all within expected and acceptable limits.

8,9-Dimethoxy-1-(3-hydroxy-4-methoxybenzyl)-4-(3,4,5-trimethoxybenzyl)-4*H*-benzo[*de*][1,6]naphthyridin-1-ium Bromide (8d**).** 4-(3,4,5-Trimethoxybenzyl)aaptamine (**7c**, 0.40 g, 0.89 mmol) was dissolved in anhydrous dimethylformamide (50 mL). Potassium carbonate (373 mg, 2.70 mmol) and 3-hydroxy-4-methoxybenzyl bromide (0.585 g, 2.70 mmol) were added. The mixture was stirred for 12 h at room temperature. Filtration and removal of the solvent in vacuo gave a yellow oil that was subjected to column chromatography (silica gel, $\text{CH}_2\text{Cl}_2/\text{CH}_3\text{OH}$ 6:1). The product was obtained as a yellow, brown oil. (0.41 g, 73%): R_f 0.39 ($\text{CH}_2\text{Cl}_2-\text{CH}_3\text{OH}$ 10:1); UV (CH_3OH) λ_{max} (log ϵ) 210 (4.56), 262 (4.29), 273 (4.27), 281 (4.27), 414 (3.79) nm; IR (KBr) ν 1647, 1587, 1568, 1510, 1460, 1425, 1244, 1126 cm^{-1} ; ^1H NMR (500 MHz, CD_3OD) δ 3.61 (s, 3H, OCH_3), 3.63 (s, 3H, OCH_3), 3.69 (s, 3H, OCH_3), 3.73 (s, 6H, 2 x OCH_3), 3.97 (s, 3H, OCH_3), 5.30 (s, 2H, NCH_2), 5.55 (s, 2H, NCH_2), 6.55 (dd, $J = 1.5$ Hz, 8.5 Hz, 1H, C_{ar}), 6.62 (d, $J = 2$ Hz, 1H, C_{ar}), 6.69 (s, 2H, C_{ar}), 6.75 (d, $J = 8.0$ Hz, 1H, H-3), 6.82 (d, $J = 8.0$ Hz, 1H, C_{ar}), 7.12 (d, $J = 7.3$ Hz, 1H, H-6), 7.35 (s, 1H, H-7), 7.80 (d, $J = 7.3$ Hz, 1H, H-5), 8.22 (d, $J = 8.0$ Hz, 1H, H-2), 9.07 (s, 1H, OH); ^{13}C NMR (126 MHz, CD_3OD) δ 55.59, 55.86, 56.02, 56.63, 58.86, 60.00, 61.37, 98.05, 98.05, 102.98, 104.99, 112.22, 113.75, 114.15, 117.13, 118.53, 129.28, 129.91, 132.46, 133.01, 134.09, 134.82, 137.32, 146.65, 147.19, 148.91, 149.40, 153.24, 158.17; EIMS m/z 544 (4), 394 (11), 213 (18), 181 (100), 137 (18), 95 (16), 94 (17), 28 (38).

Antimicrobial Susceptibility Testing. Compounds were screened against the bacteria *Stenotrophomonas maltophilia*, *Micrococcus luteus*, *Staphylococcus aureus*, *Escherichia coli*, *Enterobacter cloacae*, *Enterococcus faecalis*, *Streptococcus pneu-*

moniae, *Neisseria gonorrhoeae*, and the fungi *Candida albicans* and *Cryptococcus neoformans*, according to established broth microdilution susceptibility assays.^{32,33} The minimum inhibitory concentration was defined as the lowest concentration of compound that inhibited all visible growth of the test organism (optically clear). Assays were repeated on separate days. *Mycobacterium tuberculosis* H₃₇Rv was screened using the Microplate Alamar Blue Assay.³⁴

Results and Discussion

The 4-benzylaaptamines **7a–c** were prepared as described previously¹⁶ for the synthesis of 4-methylaaptamine (**4**). The selective benzylation of aaptamine (**1**) was achieved using sodium hexamethyldisilazane (NaHMDS) as a base and benzyl bromide, 4-methoxybenzyl bromide, or 3,4,5-methoxybenzyl bromide in tetrahydrofuran at -78 °C (Scheme 2). However, an attempt to isolate the free bases of **7a–c** using silica gel or alumina column chromatography caused some decomposition. Therefore, when the reaction was complete, dilute hydrochloric acid was added, and benzylamines **7a–c** were isolated as stable, greenish yellow hydrochloride salts in yields from 59 to 65%. The X-ray structure analysis of **7b** and **7c** showed that the benzyl group was bonded to nitrogen N-4 as we observed earlier in the case of *N*-4-methylaaptamine (**4**).

Fortunately, treatment of aaptamine (**1**) with potassium carbonate and an excess of benzyl bromide, 4-methoxybenzyl bromide, or 3,4,5-methoxybenzyl bromide in dimethylformamide led to formation of the quaternary benzo[*de*][1,6]-naphthyridinium salts **8a–c** in yields from 68 to 89%. These compounds were obtained as bright yellow crystals. Also, we were able to synthesize a naphthyridinium salt with two different benzyl units. For example, treatment of amine **7c** with 3-hydroxy-4-methoxybenzyl bromide led to formation of benzo[*de*][1,6]-naphthyridinium salt **8d**. The structures of all these derivatives were established via NMR and high-resolution mass spectral data. The structures of the naphthyridinium salts **8a–c** were all confirmed by X-ray crystallographic techniques. Surprisingly, naphthyridinium salt **8a** crystallized as a chloride salt whereas **8b** and **8c** crystallized as bromide salts. In every case, we used the hydrochloride salt of aaptamine and the corresponding benzyl bromides. It is noteworthy that **8a** crystallized directly from the reaction solution. The chloride salt of **8a** was probably less soluble than the corresponding bromide and crystallized preferentially from the reaction solution. Compounds **8b** and **8c** did not crystallize from the reaction solution and were first purified by column chromatography. These compounds therefore crystallized as bromide salts (Figures 1–5).

All of the synthetic products were evaluated against a minipanel of human cancer cell lines and the murine P388 lymphocytic leukemia cell line. These results are summarized in Tables 1. As previously published, methylation of aaptamine (**1**) at nitrogen N-4 led to an inactive derivative (**4**). However, the benzyl derivatives **7a–c** exhibited much higher cancer cell line activity than that exhibited by methylamine **4**. Within this benzyl series, amine **7b** showed good activity, whereas the activity of amine **7c** was marginal. The results in the case of the quaternary benzo[*de*][1,6]-naphthyridinium salts **5** and **8a–c** were quite similar. The

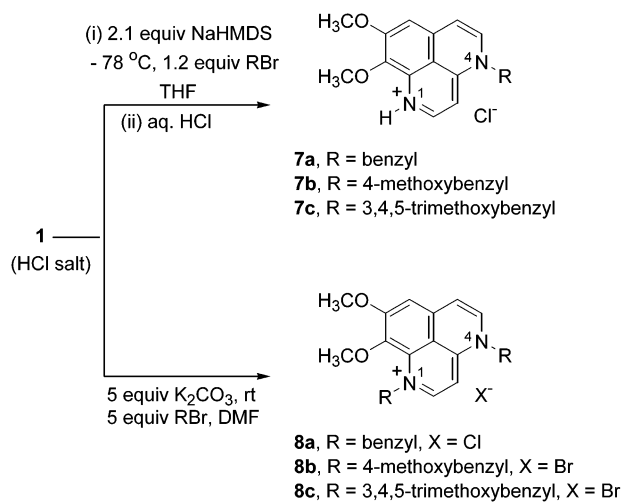
Table 1. Cell Growth Inhibitory Activity of the Synthetic Aaptamines **4**, **7a–c**, **5**, and **8a–d** (ED₅₀ μg/mL)

compound	leukemia P388	pancreas BXPC-3	breast MCF-7	CNS SF-268	lung NCI-H460	colon KM20L2	prostate DU-145
4	>10	>10	>10	>10	>10	>10	>10
7a	1.64	4.3	>10	>10	4.9	2.2	4.4
7b	2.19	4.2	8.0	8.2	5.1	3.9	3.1
7c	4.64	>10	>10	>10	>10	3.4	>10
5	3.89	7.1	4.9	0.69	>10	6.1	3.5
8a	0.234	0.061	0.27	0.064	0.26	0.055	0.036
8b	1.30	0.11	0.39	0.27	0.33	0.13	0.10
8c	>10	>10	>10	>10	>10	>10	>10
8d	>10	>10	>10	>10	>10	>10	>10

Table 2. Antimicrobial Activities of the Synthetic Aaptamines **7a–c** and **8a–d**

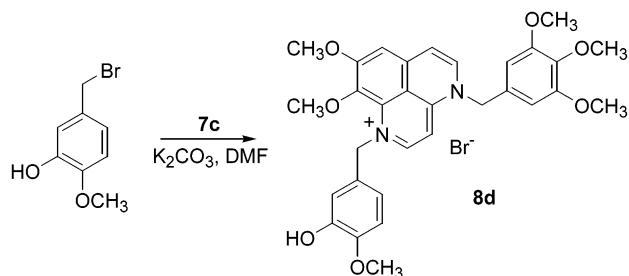
microorganism	range of min. inhibitory concn (μg/mL)						
	7a	7b	7c	8a	8b	8c	8d
<i>Cryptococcus neoformans</i>	a	a	a	a	32–64	a	a
<i>Candida albicans</i>	a	a	a	a	a	a	a
<i>Staphylococcus aureus</i>	a	a	a	a	4	a	a
<i>Streptococcus pneumoniae</i>	64	64	a	32	16–32	a	a
<i>Enterococcus faecalis</i>	a	a	a	32	16–32	a	a
<i>Micrococcus luteus</i>	a	64	a	0.5–2	<0.5	64	8–16
<i>Escherichia coli</i>	a	a	a	8	a	a	a
<i>Enterobacter cloacae</i>	a	a	a	a	a	a	a
<i>Stenotrophomonas maltophilia</i>	a	a	a	a	a	a	a
<i>Neisseria gonorrhoeae</i>	64	64	64	0.25	4	a	a

^a No inhibition at 64 μg/mL.

Scheme 2

bisbenzyl derivatives **8a** and **8b** exhibited significant inhibitory activity against the murine P388 lymphocytic leukemia and human cancer cell lines. However, the bismethyl derivative **5** was less active and salts **8c** and **8d** were inactive. In general, replacing a methyl group by a benzyl group led to an increase in the cancer cell growth inhibitory activity. Additionally, we found that increasing the number of methoxy groups in the series **7a–c** and **8a–c** led to a decrease in the cancer cell growth inhibitory activity. That was an unexpected result.

Compounds **4**, **5**, **7a–c**, and **8a–d** were evaluated as ligands for PKC, based on the initial report of activity for isoaptamine.¹⁵ Activity was measured at 30 FM compound using inhibition of [20-³H]phorbol 12,13-dibutyrate binding to PKC alpha as described previously.³⁵ Assays were carried out with triplicate measurement in either single or triplicate experiments, depending on the compound. Inhibition by **7a** and **7b**

Scheme 3

was 6.4% and 9.2%, respectively. That by **8a**, **8b**, and **8d** was 11.8%, 12.6%, and 16.0%, respectively. That by other derivatives was 5% or less. We conclude that these compounds show only very weak activity as ligands for PKC.

We further evaluated the ability of the derivatives to inhibit PKC catalytic activity. PKC alpha was stimulated in the presence of 1 FM phorbol 12-myristate 13-acetate and 100 μg/mL of phospholipid (20% phosphatidylserine: 80% phosphatidylcholine w/w) and its phosphorylation of the peptide PKC selective substrate (cat. number 527151, Calbiochem, La Jolla, CA) was determined in the presence of 30 FM compound.³⁶ Marked inhibition was observed for compounds **8a** and **8b** and lesser inhibition for **8d**. Values of percent inhibition were 71.1 ± 4.5%, 84.6 ± 1.1%, and 43.2 ± 10.1%, respectively. Inhibition by **8c** was 19.5 ± 7.6% and inhibition by **4**, **5**, and **7a, b, c** was 6% or less (all values are mean ± SEM, three experiments). For the most potent compounds, **8a** and **8b**, we additionally determined complete dose response curves for inhibition. ID₅₀ values were 20.8 ± 2.5 FM and 7.4 ± 1.2 FM, respectively (mean ± SEM, three experiments). In both cases, the inhibition curves were steeper than predicted for a competitive inhibitor, consistent with a complicated mechanism of action (Hill coefficients for **8a** and **8b** of 1.5 ± 0.1 and 2.0 ± 0.5, respectively).

A number of the aaptamine derivatives whose synthesis is described here were examined for potential effects on tubulin assembly. These were compounds **2**, **4**, **5**, **7a–c**, and **8a–d**. No significant activity was observed at the highest concentration evaluated (40 FM), except with compound **2**. This agent weakly inhibited the extent of tubulin assembly (20 min incubation at 30 °C), with an IC₅₀ value of 31 FM. For comparison, in experiments performed contemporaneously, the potent colchicine site drug combretastatin A-4 yielded an IC₅₀ value of about 2 FM. We therefore conclude that the cytotoxicity of this series of compounds does not result from an interaction with tubulin.

A flow cytometry cell cycle analysis of THP-1 human monocytic leukemia cells, stained with propidium iodide,

and pretreated for 24 h with 0.25 $\mu\text{g}/\text{mL}$ **8a**, showed an accumulation of cells in the G₁ phase. A cDNA microarray assay (BD Biosciences Clontech) with THP-1 cells treated for 23 h with 0.25 $\mu\text{g}/\text{mL}$ **8a** demonstrated significant down-regulation (5- to 7-fold) of several genes whose products are involved in DNA synthesis. These results suggest that **8a** may block the S-phase of the cell cycle.

We recently reported the antibacterial and antifungal activities of iso-aaptamine and a synthetic diphenol derivative of aaptamine.¹⁶ In the present study, benzyl derivatives **7a–c** and bisbenzyl derivatives **8c** and **8d** had only marginal antibacterial activities (Table 2). As was the case for cancer cell line inhibition, bisbenzyl derivatives **8a** and **8b** demonstrated the most promising antibacterial profiles (Table 2). In addition, **8b** had antifungal activity (Table 2). Derivatives **7a–c** and **8a–d** were also evaluated against *Mycobacterium tuberculosis*. At 6.25 $\mu\text{g}/\text{mL}$, compounds **8a** and **8b** were active, exhibiting 98% and 97% inhibition, respectively.

In conclusion, convenient syntheses of a selection of benzylaaptamines have been developed. We were pleased to discover that some of these compounds exhibited significant anticancer and antimicrobial activities, in particular compound **8a**.

Acknowledgment. The very helpful financial assistance was provided by Outstanding Investigator Grant CA44344-05-12 and grant RO1 CA90441-01 awarded by the Division of Cancer Treatment and Diagnosis, National Cancer Institute DHHS; the Arizona Disease Control Research Commission; the Fannie E. Rippel Foundation; the Robert B. Dalton Endowment Fund; the Caitlin Robb Foundation; Gary L. and Diane Tooker; Polly J. Trautman; Billie Jane Baguley; Lotte Flugel; Dr. John C. Budzinski; the Eagles Art Ehrmann Cancer Fund; and the Ladies Auxiliary to the Veterans of Foreign Wars. For other helpful assistance, we thank Drs. Jean-Charles Chapuis and Fiona Hogan, Mr. Lee Williams, Ms. Natalie Fuller, and Ms. Bridget Fakoury. Antimicrobial data were provided by the Tuberculosis Antimicrobial Acquisition and Coordinating Facility (TAACF) through a research and development contract with the U.S. National Institute of Allergy and Infectious Diseases.

Supporting Information Available: Crystallographic data containing fractional coordinates, isotropic and anisotropic displacement parameters, and bond lengths and angles for **7b,c** and **8a–c**. This material is available free of charge via the Internet at <http://pubs.acs.org>.

References

- For contribution 498 refer to Bai, R.; Bates, R. B.; Hamel, E.; Moore, R. E.; Nakkiew, P.; Pettit, G. R.; Sufi, B. A. *J. Nat. Prod.* **2002**, *65*, 1824–1829.
- Li, J.; Burgett, A. W. G.; Esser, L.; Amezcua, C.; Harran, P. G. Total Synthesis of Nominal Diazonamides – Part 2: On the true Structure and Origin of Natural Isolates. *Angew. Chem., Int. Ed.* **2001**, *40*, 4770–4773.
- Kinder, F. R.; Versace, R. W.; Bair, K. W.; Bontempo, J. M.; Cesarz, D.; Chen, S.; Crews, P.; Czuchta, A. M.; Jagoe, C. T.; Mou, Y.; Nemzek, R.; Phillips, P. E.; Tran, L. D.; Wang R–M.; Weltchek, S.; Zabudoff, S. Synthesis and Antitumor Activity of Ester-Modified Analogues of Bengamide B. *J. Med. Chem.* **2001**, *44*, 3692–3699.
- Casapullo, A.; Cutignano, A.; Bruno, I.; Bifulco, G.; Debitus, C.; Gomez-Paloma, L.; Riccio, R. Makaluvamine P, a New Cytotoxic Pyrroloiminoquinone from *Zyzya cf. fuliginosa*. *J. Nat. Prod.* **2001**, *64*, 1354–1356.
- Grassia, A.; Bruno, I.; Debitus, C.; Marzocco, S.; Pinto, A.; Gomez-Paloma, L.; Riccio, R. Spongidepsin, a New Cytotoxic Macrolide from *Spongia* sp. *Tetrahedron* **2001**, *57*, 6257–6260.
- Zhou, B.-N.; Slebodnick, C.; Johnson, R. K.; Mattern, M. R.; Kingston, D. G. I. New Cytotoxic Manzamine Alkaloids from a Palaun Sponge. *Tetrahedron* **2000**, *56*, 5781–5784.
- Zampella, A.; Giannini, C.; Debitus, C.; D'Auria, M. V. Amphisterins: a New Family of Cytotoxic Metabolites from the Marine Sponge *Plakortis quasiamphister*. *Tetrahedron* **2001**, *57*, 257–263.
- Hirano, K.; Kubota, T.; Tsuda, M.; Mikami, Y.; Kobayashi, J. Pyridodems B–D, Potent Cytotoxic Bis-pyridine Alkaloids from Marine Sponge *Amphimedon* sp. *Chem. Pharm. Bull.* **2000**, *48*, 974–977.
- Nakamura, H.; Kobayashi, J.; Ohizumi, Y.; Hirata, Y. Isolation and Structure of Aaptamine, a Novel Heteroaromatic Substance Possessing α -Blocking Activity from the Sea Sponge *Aaptos aaptos*. *Tetrahedron Lett.* **1982**, *23*, 5555–5558.
- Ohizumi, Y.; Kajiwara, A.; Nakamura, H.; Kobayashi, J. Alpha-Adrenoceptor Blocking Action of Aaptamine, a Novel Marine Natural Product, in Vascular Smooth Muscle. *J. Pharm. Pharmacol.* **1984**, *36*, 785–786.
- Fedoreev, S. A.; Prokofeva, N. G.; Denisenko, V. A.; Rebachuk, N. M. Cytotoxic Activity of Aaptamines Derived from Suberitidae Sponges. *Khimiko-Farmatsevticheskii Zhurnal* **1988**, *22*, 943–946.
- Kashman, Y.; Rudi, A.; Hirsch, S.; Isaacs, S.; Green, D.; Blasberger, D.; Carmely, S. Recent Developments in Research on Metabolites from Red Sea Invertebrates. *New J. Chem.* **1990**, *14*, 729–740.
- Shen, Y.-C.; Chein, C.-C.; Hsieh, P.-W.; Duh, C.-Y. Bioactive Constituents from Marine Sponge *Aaptos aaptos*. *Taiwan Shuichan Xuehuikan* **1997**, *24*, 117–125.
- Pettit, G. R.; Hoffmann, H.; Murphy, A.; Malloy, D.; McNulty, J.; Higgs, K. C.; Herald, D. L.; Williams, M. D.; Boyd, M. R.; Pettit, R. K.; Doubek, D. L.; Hooper, J. N. A.; Tackett, R. P.; Albright, L.; Schmidt, J. M. Antineoplastic Agents 380. Isolation and X-ray Crystal Structure Determination of Isoaaptamine from the Republic of Singapore Hymeniacidon sp. and Conversion to the Prodrug Hystatin. *J. Nat. Prod.*, in press.
- Patil, A. D.; Westley, J. W.; Mattern, M.; Freyer, A. J.; Hofmann, G. A. Aaptamines as Protein Kinase C Inhibitors. *PCT Int. Appl. WO 95/0584*, 1995.
- Pettit, G. R.; Hoffmann, H.; Herald, D. L.; McNulty, J.; Murphy, A.; Higgs, K. C.; Lewin, N. E.; Blumberg, P. M.; Pettit, R. K.; Knight, J. C. Antineoplastic Agents 491. Synthetic Conversion of Aaptamine to Isoaaptamine and 9-Demethylaaptamine. *J. Org. Chem.*, in press.
- Shen, Y.-C.; Lin T–T.; Sheu, J.-H.; Duh, C.-Y. Structures and Cytotoxicity Relationship of Isoaaptamine and Aaptamine Derivatives. *J. Nat. Prod.* **1999**, *62*, 1264–1267.
- Sugino, E.; Choshi, T.; Hibino, S. Progress in Total Synthesis of Marine Alkaloids, Aaptamine. *Heterocycles* **1999**, *50*, 543–559.
- Walz, A. J.; Sundberg, R. J. Synthesis of 8-Methoxy-1-methyl-1H-benzo[de][1,6]naphthyridin-9-ol (Isoaaptamine) and Analogues. *J. Org. Chem.* **2000**, *65*, 8001–8010.
- Hallock, Y. F.; Cardellina, J. H. II; Kornek, T.; Gulden, K.-P.; Bringmann, G.; Boyd, M. R. Gentrymine B, the First Quaternary Isoquinoline Alkaloid from *Ancistrocladus korupensis*. *Tetrahedron Lett.* **1995**, *36*, 4753–4756.
- Mitscher, L. A.; Bathala, M. S.; Beal, J. L. Antibiotics from Higher Plants: Pteleatinum Chloride, a new Quaternary Quinoline Alkaloid from *Ptelea trifoliata* with Antitubercular and Antiyeast activity. *J. Chem. Soc., Dalton Trans.* **1971**, *17*, 1040–1040.
- Psotova, J.; Ducher, L.; Ulrichova, J.; Waltierova, D. Quaternary Isoquinoline Alkaloids as Protein Kinase C Inhibitors. *Chemické Listy* **1996**, *90*, 613–614.
- Del Poeta, M.; Chen, S.-F.; Von Hoff, D.; Dykstra, C. C.; Wani, M. C.; Manikumar, G.; Heitman, J.; Wall, M. E.; Perfect, J. R. Comparison of In Vitro Activities of Camptothecin and Nitidine Derivatives against Fungal and Cancer Cells. *Antimicrob. Agents Chemother.* **1999**, *43*, 2862–2868.
- Tan, G. T.; Pezzuto, J. M.; Kinghorn, A. D.; Hughes, S. H. Evaluation of Natural Products as Inhibitors of Human Immunodeficiency Virus Type 1 (HIV-1) Reverse Transcriptase. *J. Nat. Prod.* **1991**, *54*, 143–154.
- Yang, S. S.; Cragg, G. M.; Newman, D. J.; Bader, J. P. Natural Product-Based Anti-HIV Drug Discovery and Development Facilitated by the NCI Developmental Therapeutics Program. *J. Nat. Prod.* **2001**, *64*, 265–277.
- Kanzawa, F.; Nishio, K.; Ishida, T.; Fukuda, M.; Kurokawa, H.; Fukumoto, H.; Nomoto, Y.; Fukuoka, K.; Bojanowski, K.; Saijo, N. Antitumor Activities of a New Benzocyclohexanthridine Agent, 2,3-(Methylenedioxy)-5-methyl-7-hydroxy-8-methoxybenzo[c]-phenanthridinium Hydrogen Sulfate Dihydrate (NK109), against Several Drug-Resistant Human Tumor Cell Lines. *Br. J. Cancer* **1997**, *76*, 571–581.

- (27) Pinney, K. G.; Mejia, M. P.; Villalobos, V. M.; Rosenquist, B. E.; Pettit, G. R.; Verdier-Pinard, P.; Hamel, E. Synthesis and Biological Evaluation of Aryl Azide Derivatives of Combretastatin A-4 as Molecular Probes for Tubulin. *Bioorg. Med. Chem.* **2000**, *8*, 2417–2425.
- (28) SMART for Windows NT v5.605; BrukerAXS Inc.: Madison, WI, 2000.
- (29) XPREP—The automatic space group determination program in the SHELXTL (see ref 31).
- (30) Blessing, R. H. An Empirical Correction for Absorption Anisotropy. *Acta Crystallogr.* **1995**, *A51*, 33–38.
- (31) SHELXTL-NT Version 5.10; Bruker AXS Inc.: Madison, WI, 1997. An integrated suite of programs for the determination of crystal structures from diffraction data. This package includes, among others, XPREP (an automatic space group determination program), SHELXS (a structure solution program via Patterson or direct methods), and SHELXL (structure refinement software).
- (32) National Committee for Clinical Laboratory Standards. Methods for Dilution Antimicrobial Susceptibility Tests for Bacteria that Grow Aerobically. Approved Standard M7-A4. Wayne, PA: NCCLS, 1997.
- (33) National Committee for Clinical Laboratory Standards. Reference Method for Broth Dilution Antifungal Susceptibility Testing of Yeasts. Approved Standard M27-A. Wayne, PA: NCCLS, 1997.
- (34) Collins, L.; Franzblau, S. G. Microplate Alamar Blue Assay Versus BACTEC 460 System for High-throughput Screening of Compounds against *Mycobacterium tuberculosis* and *Mycobacterium avium*. *Antimicrob. Agents Chemother.* **1997**, *41*, 1004–1009.
- (35) Kazanietz, M. G.; Areces, L. B.; Bahador, A.; Mischak, H.; Goodnight, J.; Mushinski, J. F.; Blumberg, P. M. Characterization of Ligand and Substrate Specificity for the Calcium-Dependent and Calcium-Independent Protein Kinase C Isoenzymes. *Molecular Pharmacol.* **1993**, *44*, 298–307.
- (36) Nacro, K.; Bienfait, B.; Lee, J.; Han, K. C.; Kang, J. H.; Benzaria, S.; Lewin, N. E.; Bhattacharyya, D.; Blumberg, P. M.; Marquez, V. E. Conformationally Constrained Analogues of Diacylglycerol (DAG). 16. How Much Structural Complexity is Necessary for Recognition and High Binding Affinity to Protein Kinase C? *J. Med. Chem.* **2000**, *43*, 921–944.

JM030070R